IEEE *Access*

Hybrid Tightly-coupled SINS/LBL for Underwater Navigation System

LING ZHOU[1], YIXIAN ZHU[2]

[1]Department of Physics and Electronic Engineering, Yuncheng University, Yuncheng 044000, China
[2]Department of Materials Science and Engineering, Nantong University, Nantong 226019, China

Corresponding author: Ling Zhou (s03031212@126.com)

ABSTRACT The application of long baseline aided strap-down inertial navigation system (SINS/LBL) has been demonstrated to be an effective solution for accumulative position errors of underwater vehicles (UVs). To address the inefficient positioning when available hydrophones are few in acoustic array, a hybrid tightly-coupled SINS/LBL is presented for underwater navigation system. The system is composed of SINS, LBL and pressure sensor (PS). The hybrid positioning model based on slant range, slant-range rate, slant-range difference and slant-range rate difference is established according to the location principle of time of arrival (TOA) and time difference of arrival (TDOA) when the number of available hydrophones is two. TDOA positioning model based on slant-range difference and slant-range rate difference is adopted when the number of available hydrophones is more than two. The two tightly-coupled SINS/LBL models could be switched with each other as the number of available hydrophones changes in acoustic array. This paper used experimental data obtained from an unmanned surface vehicle (USV) to validate the navigation performance. Compared with single tightly-coupled SINS/LBL model, the proposed method can provide faster error convergence and more accurate submerged position fixes.

INDEX TERMS Hybrid positioning, tightly-coupled, long baseline, integrated navigation, underwater vehicle

I. INTRODUCTION

Modern ocean technology has become a research hotspot in the field of latest technology with the exploration of ocean resource and the utilization of ocean energy. Underwater vehicles (UVs) are important tools to complete underwater sampling, monitoring and exploration [1]. Underwater navigation and positioning are the prerequisites for the UVs' normal operation [2]. High accuracy is a key specification of underwater navigation in long duration. However, under the influence of complex underwater environment, accurate underwater navigation has always been one of the difficulties for UVs. At present, strap-down inertial navigation system (SINS), acoustic navigation and geophysical navigation are taken as common approaches for underwater navigation and positioning technology [3,4]. Various navigation methods have their own advantages and disadvantages, and they complement each other in specific applications [5,6]. For different tasks and operations of UVs, Doppler velocity log

(DVL) aided SINS (SINS/DVL) is always taken as the primary navigation system, but SINS/DVL can hardly meet the requirements of underwater navigation for long-range UVs on the principle of dead reckoning even with the high-precision SINS and DVL. Furthermore, to address the accumulative errors by dead reckoning and to enhance the accuracy of underwater navigation and positioning for long-range UVs, they require other auxiliary navigation methods, such as global navigation satellite system (GNSS) [7], acoustic navigation [8-12], geophysical navigation [4,13], magnetic compass (MCP) and pressure sensor (PS) [14].

GNSS is a popular positioning approach for air, land and shallow sea because of its global, all-weather and high-accuracy characteristics. When the vehicle moored on the mother ship is ready for missions, its initial position is obtained via GNSS at surface. Although for many advantages, GNSS cannot directly access to deep sea due to rapid radio attenuation. Acoustic navigation is well known as

a viable alternative to GNSS for deep-water applications accounting for underwater acoustic propagation characteristics. Long baseline (LBL), short baseline (SBL) and ultrashort baseline (USBL) are main acoustic navigation methods to provide appropriate geometric constraints on the vehicle's position estimate [2,3]. Here, we concentrate on LBL-aided SINS (SINS/LBL) suitable for small UVs. LBL is analogous to an underwater GNSS system. On the basis of the principle of geometric positioning, it is crucial that the time-of-flight (TOF) measurement errors are within an acceptable tolerance between the transmitter and receiver. Thus, there are two common ways to measure TOF, i.e. the time of arrival (TOA) [15,16] and the time difference of arrival (TDOA) [17]. Lee et al. [8,9,15] proposed an integrated navigation system based on SINS accompanying range sensor, DVL, MCP and depth sensor. Pseudo LBL system which is consisted of one or two transducers measured the distance from the vehicle to an underwater reference station for range aiding (RA) or range phase aiding (RPA). To address the difficulties in launching and recovering the transponders, it employed one or two acoustic transponders (reference station). Webster et al. [10] used a single moving reference beacon to measure range based on one-way TOF. The maximum operating range value is set to solve incorrect TOF measurement caused by acoustic multipath propagation or reflection. Kepper et al. [11] researched and applied single-beacon one-way TOF acoustic navigation to low-cost underwater vehicle navigation with MEMS IMU, model-based velocity and acoustic range measurements.

Because the TOA is based on the difference between the transmitter's time and the receiver's time, it requires synchronized clocks on both the transmitter and the receiver, while it only needs synchronized clocks on the reference beacons (in our case the hydrophones) in the TDOA. Zhang et al. [17-19] studied the tightly-coupled SINS/LBL based on TDOA positioning model. The TDOA is changed into slant-range difference. Underwater acoustic propagation multipath and sound velocity calculation are solved through interactive assistance of SINS and LBL. Recent advances in acoustic navigation methods are enabling extended UVs' mission. This paper builds upon the research in TOA and TDOA acoustic navigation for measurements to determine UVs position. Taking advantages of TOA and TDOA, a hybrid tight-coupled SINS/LBL model is proposed for providing rapid error convergence and positioning when the vehicle enters the acoustic array area. Additionally, PS is one of the common devices for UVs because of its high-reliability and low-cost, and suitable for aiding rapid positioning when there are few hydrophones available. Combined with depth measurement to limit vertical divergence of SINS, using slant range measurements and slant-range rate measurements, the proposed hybrid model will be able to improve the single tightly-coupled SINS/LBL model and useful even without DVL and MCP information.

In the remainder of this paper, Section 2 presents the hybrid tightly-coupled model of SINS/LBL system. The proposed system structure and experimental setup are reported in Section 3. Section 4 discusses and analyzes the performance of the proposed method through experimental results. Finally, a relative conclusion is drawn in Section 5.

II. HYBRID TIGHTLY-COUPLED SINS/LBL MODEL

A LBL system contains a sound source on the vehicle and several hydrophones on the seafloor. The distance between the hydrophones is about from 100 m to 6000 m in general [17]. The structure and operational concept of LBL system are shown in Fig. 1.
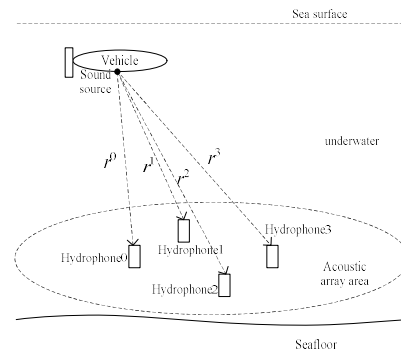

FIGURE 1. Structure of LBL system

In this section, the positioning method based on hybrid tightly-coupled SINS/LBL is proposed. In order to make full use of LBL information, the proposed hybrid model combines TOA positioning model and TDOA positioning model. The two tightly-coupled SINS/LBL models, i.e. the hybrid model and single TDOA model, could be switched with each other as the number of available hydrophones changes in acoustic array.

A. STATE-SPACE MODEL

State variables of the tightly-coupled system include errors of SINS, LBL and PS. The state equation is expressed as follows:

$$\begin{bmatrix} \dot{X}_I \\ \dot{X}_L \\ \dot{X}_P \end{bmatrix} = \begin{bmatrix} F_I & 0 & 0 \\ 0 & F_L & 0 \\ 0 & 0 & F_P \end{bmatrix} \begin{bmatrix} X_I \\ X_L \\ X_P \end{bmatrix} + \begin{bmatrix} W_I \\ W_L \\ W_P \end{bmatrix} \qquad (1)$$

where

X_I, X_L and X_P are the system state vectors of SINS, LBL and PS, respectively;

F_I, F_L and F_P are the system matrixes of SINS, LBL and PS, respectively;

W_I, W_L and W_P are the system noises of SINS, LBL and PS, respectively, which represent the instrument noise together with any unmodelled biases, and so we model the W_I, W_L and W_P as being normally distributed with a mean of zeros and some variance, i.e. $\sim \mathcal{N}(0, Q)$. Q is an invertible

covariance matrix.

X_I is denoted as:

$$X_I = [\phi_E \quad \phi_N \quad \phi_U \quad \delta v_E \quad \delta v_N \quad \delta v_U \quad \delta L \\ \delta\lambda \quad \delta h \quad \varepsilon_x \quad \varepsilon_y \quad \varepsilon_z \quad \nabla_x \quad \nabla_y \quad \nabla_z]^T \quad (2)$$

where

ϕ_E, ϕ_N and ϕ_U are misalignment angles of SINS toward east, north and the local vertical (up), respectively;

δv_E, δv_N and δv_U are velocity errors of SINS toward east, north and up, respectively;

δL, $\delta\lambda$ and δh are SINS latitude error, longitude error and depth error, respectively;

ε_x, ε_y and ε_z are three axial drifts of gyroscopes, respectively;

∇_x, ∇_y and ∇_z are three axial biases of accelerometers, respectively;

The expression of F_I can be determined by the SINS error equations in [20]. The upper dot on the top of the variables denotes the time derivatives of the variables with respect to the navigation frame.

According to the location principle of LBL, the time-dependent errors are chosen here as LBL state variables. Underwater noise, reverberation, acoustic multipath propagation, Doppler effect and other factors could impact on navigation performance, and hence LBL model is simplified by a first-order Gauss-Markov process [17-19]. More specifically, δt_j and δf_j are taken as state variables of the TOA positioning model, and then δt_{jk} and δf_{jk} are state variables of the TDOA positioning model. The detailed models are expressed as:

$$\begin{cases} \delta \dot{t}_j = \delta f_j + w_{tj} \\ \delta \dot{f}_j = -\dfrac{1}{\tau_{fj}}\delta f_j + w_{fj} \end{cases} \quad (3)$$

where

The subscript letter j is the hydrophone number;

δt_j is error of propagation time from sound source to hydrophone j;

δf_j is the rate of δt_j;

w_{tj} is driven white noise of δt_j;

τ_{fj} and w_{fj} are correlation time and driven white noise of δf_j respectively in the first-order Gauss-Markov process.

$$\begin{cases} \delta \dot{t}_{jk} = \delta f_{jk} + w_{\delta t} \\ \delta \dot{f}_{jk} = -\dfrac{1}{\tau_{\delta f}}\delta f_{jk} + w_{\delta f} \end{cases} \quad (4)$$

where

The subscript letter k is also the hydrophone number, but k is not equal to j, i.e. $k \neq j$;

δt_{jk} is error of propagation time difference between sound source to hydrophone j and to hydrophone k;

δf_{jk} is the rate of δt_{jk};

$w_{\delta t}$ is driven white noise of δt_{jk};

$\tau_{\delta f}$ and $w_{\delta f}$ are correlation time and driven white noise of δf_{jk} respectively in the first-order Gauss-Markov process.

Thus, the state vector of LBL is denoted as:

$$X_L = [\delta t_j \quad \delta f_j \quad \delta t_{jk} \quad \delta f_{jk}]^T \quad (5)$$

and the system matrix of LBL is written as:

$$F_L = \begin{bmatrix} 0 & 1 & 0 & 0 \\ 0 & -\dfrac{1}{\tau_{fj}} & 0 & 0 \\ 0 & 0 & 0 & 1 \\ 0 & 0 & 0 & -\dfrac{1}{\tau_{\delta f}} \end{bmatrix} \quad (6)$$

Accounting for seawater density, salinity and temperature, PS has nonlinear error and scale factor error. The depth error of PS can be approximated as a first-order Gauss-Markov process after error compensation. The state equation of PS depth error is expressed as follows:

$$\delta \dot{h}_p = -\frac{1}{\tau_p}\delta h_p + w_p \quad (7)$$

where δh_p is depth error of PS; τ_p and w_p are correlation time and driven white noise of the depth error respectively in the first-order Gauss-Markov process. Thus, the state vector of PS is denoted as:

$$X_P = \delta h_p \quad (8)$$

and the system matrix of PS is written as:

$$F_P = -\frac{1}{\tau_p} \quad (9)$$

B. MEASUREMENT MODEL

The vehicle position estimated by SINS is expressed as (x_I, y_I, z_I). The position of hydrophone is assumed to be known and expressed as (x_a, y_a, z_a). Furthermore, slant range and slant-range difference are calculated as [17]:

$$\rho_I^j = \sqrt{\left(x_I - x_a^j\right)^2 + \left(y_I - y_a^j\right)^2 + \left(z_I - z_a^j\right)^2} \quad (10)$$

where the subscript letter I indicates that the variable is calculated by SINS; ρ_I^j is slant range between the vehicle and hydrophone j.

$$\rho_I^{jk} = \rho_I^j - \rho_I^k \\ = \sqrt{\left(x_I - x_a^j\right)^2 + \left(y_I - y_a^j\right)^2 + \left(z_I - z_a^j\right)^2} \\ - \sqrt{\left(x_I - x_a^k\right)^2 + \left(y_I - y_a^k\right)^2 + \left(z_I - z_a^k\right)^2} \quad (11)$$

where ρ_I^{jk} is slant-range difference between the vehicle to hydrophone j and to hydrophone k.

Nonlinear Equation (10) and Equation (11) are linearized by Taylor series at the real vehicle position (x,y,z), respectively, then the linear equations are:

$$\rho_I^j = r^j + e_x^j \delta x + e_y^j \delta y + e_z^j \delta z \quad (12)$$

where

$$r^j = \sqrt{\left(x - x_a^j\right)^2 + \left(y - y_a^j\right)^2 + \left(z - z_a^j\right)^2}$$ is the real distance

between the vehicle and hydrophone j;

$e_x^j = \dfrac{x - x_a^j}{r^j}$, $e_y^j = \dfrac{y - y_a^j}{r^j}$, and $e_z^j = \dfrac{z - z_a^j}{r^j}$ are three axial

cosines of the vehicle relative to hydrophone j in rectangular coordinate;

$\delta x = x_I - x$, $\delta y = y_I - y$, $\delta z = z_I - z$ are three axial position errors in rectangular coordinate.

$$\rho_I^{jk} = r^j - r^k + e_x^{jk}\delta x + e_y^{jk}\delta y + e_z^{jk}\delta z \tag{13}$$

where

$$r^k = \sqrt{\left(x - x_a^k\right)^2 + \left(y - y_a^k\right)^2 + \left(z - z_a^k\right)^2} \quad \text{is the real}$$

distance from the vehicle to hydrophone k;

$e_x^{jk} = \dfrac{x - x_a^j}{r^j} - \dfrac{x - x_a^k}{r^k}$, $e_y^{jk} = \dfrac{y - y_a^j}{r^j} - \dfrac{y - y_a^k}{r^k}$, and

$e_z^{jk} = \dfrac{z - z_a^j}{r^j} - \dfrac{z - z_a^k}{r^k}$ are three axial cosine differences of

the vehicle relative to hydrophone j and to hydrophone k in rectangular coordinate.

There is a relative motion between the vehicle and hydrophones. The slant-range rate and slant-range rate difference of the vehicle relative to the hydrophones are obtained by taking the first derivative of slant range and slant-range difference versus three axes, respectively. The two rates are expressed as:

$$\dot{\rho}_I^j = \dot{r}^j + e_x^j\delta\dot{x} + e_y^j\delta\dot{y} + e_z^j\delta\dot{z} \tag{14}$$

where $\dot{\rho}_I^j$ is slant-range rate of the vehicle relative to hydrophone j.

$$\dot{\rho}_I^{jk} = \dot{r}^j - \dot{r}^k + e_x^{jk}\delta\dot{x} + e_y^{jk}\delta\dot{y} + e_z^{jk}\delta\dot{z} \tag{15}$$

where $\dot{\rho}_I^{jk}$ is slant-range rate difference between the vehicle relative to hydrophone j and to hydrophone k.

These four measurement variables output by LBL are expressed as:

$$\rho_L^j = r^j + c\delta t_j + \upsilon_\rho \tag{16}$$

where the subscript letter L indicates that the variable is obtained by LBL; $\rho_L^j = c\tau_j$; c is sound velocity; τ_j is propagation delay from sound source to hydrophone j; υ_ρ is measurement noise of ρ_L^j.

$$\dot{\rho}_L^j = \dot{r}^j + c\delta f_j + \upsilon_{\dot{\rho}} \tag{17}$$

where $\dot{\rho}_L^j = -\lambda f_d^j$; f_d^j is Doppler shift; λ is phase wavelength; $\upsilon_{\dot{\rho}}$ is measurement noise of $\dot{\rho}_L^j$.

$$\rho_L^{jk} = r^j - r^k + c\delta t_{jk} + \upsilon_{\delta\rho} \tag{18}$$

where $\rho_L^{jk} = c\tau_{jk}$; τ_{jk} is delay difference between sound source to hydrophone j and to hydrophone k; $\upsilon_{\delta\rho}$ is measurement noise of ρ_L^{jk}.

$$\dot{\rho}_L^{jk} = \dot{r}^j - \dot{r}^k + c\delta f_{jk} + \upsilon_{\delta\rho} \tag{19}$$

where $\dot{\rho}_L^{jk} = -\lambda f_d^{jk}$; f_d^{jk} is Doppler shift difference; $\upsilon_{\delta\rho}$ is measurement noise of $\dot{\rho}_L^{jk}$.

By the analysis of measurement variables, the measurement equations are written as follows:

The measurement equation of slant-range difference is:

$$\begin{aligned} \delta\rho^j &= \rho_I^j - \rho_L^j = e_x^j\delta x + e_y^j\delta y + e_z^j\delta z - c\delta t_j - \upsilon_\rho \\ &= [e_x^j \quad e_y^j \quad e_z^j \quad -c][\delta x \quad \delta y \quad \delta z \quad \delta t_j]^T - \upsilon_\rho \end{aligned} \tag{20}$$

$C_{L\lambda h}^{ECEF}$ is a transfer matrix from geodetic coordinate to rectangular coordinate. It is expressed as:

$$C_{L\lambda h}^{ECEF} = \begin{bmatrix} -(R_M + h)\sin L\cos\lambda & -(R_M + h)\cos L\sin\lambda & \cos L\cos\lambda \\ -(R_M + h)\sin L\sin\lambda & (R_M + h)\cos L\cos\lambda & \cos L\sin\lambda \\ \left[R_M\left(1 - e^2\right) + h\right]\cos L & 0 & \sin L \end{bmatrix} \tag{21}$$

where

R_M is the transverse radius of curvature;

L, λ and h are SINS latitude, longitude and depth, respectively;

e represents the major eccentricity of the ellipsoid.

The transfer matrix $C_{L\lambda h}^{ECEF}$ is introduced into Equation (20), and then the measurement equation of slant-range difference becomes:

$$\mathbf{Z}_\rho = \mathbf{H}_\rho \mathbf{X} + \mathbf{V}_\rho \tag{22}$$

where $\mathbf{Z}_\rho = [\delta\rho^j]_{N\times 1}$; $\mathbf{H}_\rho = [\mathbf{0}_{N\times 6} \quad \mathbf{H}_{\rho 1} \quad \mathbf{0}_{N\times 6} \quad \mathbf{H}_{\rho 2} \quad \mathbf{0}_{N\times 3}]$; $\mathbf{H}_{\rho 1} = [e_x^j \quad e_y^j \quad e_z^j]_{N\times 3} C_{L\lambda h}^{ECEF}$; $\mathbf{H}_{\rho 2} = [-c \quad 0]_{N\times 2}$; $\mathbf{V}_\rho = [-\upsilon_\rho]_{N\times 1}$; N is the number of available hydrophones; Here, N=2.

The measurement equation of slant-range rate difference is:

$$\begin{aligned} \delta\dot{\rho}^j &= \dot{\rho}_I^j - \dot{\rho}_L^j = e_x^j\delta\dot{x} + e_y^j\delta\dot{y} + e_z^j\delta\dot{z} - c\delta f_j - \upsilon_{\dot{\rho}} \\ &= [e_x^j \quad e_y^j \quad e_z^j \quad -c][\delta\dot{x} \quad \delta\dot{y} \quad \delta\dot{z} \quad \delta f_j]^T - \upsilon_{\dot{\rho}} \end{aligned} \tag{23}$$

C_{ENU}^{ECEF} is a transfer matrix from local geographic coordinate to rectangular coordinate. Here, the origin of the geographic coordinate is at the location of the navigation system, and its axes are aligned with the directions of east, north, and up. C_{ENU}^{ECEF} is:

$$C_{ENU}^{ECEF} = \begin{bmatrix} -\sin\lambda & -\sin L\cos\lambda & \cos L\cos\lambda \\ \cos\lambda & -\sin L\sin\lambda & \cos L\sin\lambda \\ 0 & \cos L & \sin L \end{bmatrix} \tag{24}$$

The transfer matrix C_{ENU}^{ECEF} is introduced into Equation (23), and then the measurement equation of slant-range rate difference becomes:

$$\boldsymbol{Z}_{\dot\rho} = \boldsymbol{H}_{\dot\rho}\boldsymbol{X} + \boldsymbol{V}_{\dot\rho} \qquad (25)$$

where $\boldsymbol{Z}_{\dot\rho} = [\delta\dot\rho^{j}]_{N\times1}$; $\boldsymbol{H}_{\dot\rho} = [\boldsymbol{0}_{N\times3} \quad \boldsymbol{H}_{\dot\rho1} \quad \boldsymbol{0}_{N\times9} \quad \boldsymbol{H}_{\dot\rho2} \quad \boldsymbol{0}_{N\times3}]$; $\boldsymbol{H}_{\dot\rho1} = [e_x^{j} \quad e_y^{j} \quad e_z^{j}]_{N\times3} C_{ENU}^{ECEF}$; $\boldsymbol{H}_{\dot\rho2} = [0 \quad -c]_{N\times2}$; $V_{\dot\rho} = [-\upsilon_{\dot\rho}]_{N\times1}$; N=2.

The measurement equation of the difference of slant-range difference is:

$$\delta\rho^{jk} = \rho_I^{jk} - \rho_L^{jk} = e_x^{jk}\delta x + e_y^{jk}\delta y + e_z^{jk}\delta z - c\delta t_{jk} - \upsilon_{\delta\rho}$$
$$= [e_x^{jk} \quad e_y^{jk} \quad e_z^{jk} \quad -c][\delta x \quad \delta y \quad \delta z \quad \delta t_{jk}]^T - \upsilon_{\delta\rho} \qquad (26)$$

The transfer matrix $C_{L\lambda h}^{ECEF}$ is introduced into Equation (26), and then the measurement equation of the difference of slant-range difference becomes:

$$\boldsymbol{Z}_{\delta\rho} = \boldsymbol{H}_{\delta\rho}\boldsymbol{X} + \boldsymbol{V}_{\delta\rho} \qquad (27)$$

where $\boldsymbol{Z}_{\delta\rho} = [\delta\rho^{jk}]_{(N-1)\times1}$; $\boldsymbol{H}_{\delta\rho} = [\boldsymbol{0}_{(N-1)\times6} \quad \boldsymbol{H}_{\delta\rho1} \quad \boldsymbol{0}_{(N-1)\times8} \quad \boldsymbol{H}_{\delta\rho2} \quad \boldsymbol{0}_{(N-1)\times1}]$; $\boldsymbol{H}_{\delta\rho1} = [e_x^{jk} \quad e_y^{jk} \quad e_z^{jk}]_{(N-1)\times3} C_{L\lambda h}^{ECEF}$; $\boldsymbol{H}_{\delta\rho2} = [-c \quad 0]_{(N-1)\times2}$; $V_{\delta\rho} = [-\upsilon_{\delta\rho}]_{(N-1)\times1}$; $N{\geq}2$.

The measurement equation of the difference of slant-range rate difference is:

$$\delta\dot\rho^{jk} = \dot\rho_I^{jk} - \dot\rho_L^{jk} = e_x^{jk}\delta\dot x + e_y^{jk}\delta\dot y + e_z^{jk}\delta\dot z - c\delta f_{jk} - \upsilon_{\delta\dot\rho}$$
$$= [e_x^{jk} \quad e_y^{jk} \quad e_z^{jk} \quad -c][\delta\dot x \quad \delta\dot y \quad \delta\dot z \quad \delta f_{jk}]^T - \upsilon_{\delta\dot\rho} \qquad (28)$$

The transfer matrix C_{ENU}^{ECEF} is introduced into Equation (28), and then the measurement equation of the difference of slant-range rate difference becomes:

$$\boldsymbol{Z}_{\delta\dot\rho} = \boldsymbol{H}_{\delta\dot\rho}\boldsymbol{X} + \boldsymbol{V}_{\delta\dot\rho} \qquad (29)$$

where $\boldsymbol{Z}_{\delta\dot\rho} = [\delta\dot\rho^{jk}]_{(N-1)\times1}$; $\boldsymbol{H}_{\delta\dot\rho} = [\boldsymbol{0}_{(N-1)\times3} \quad \boldsymbol{H}_{\delta\dot\rho1} \quad \boldsymbol{0}_{(N-1)\times11} \quad \boldsymbol{H}_{\delta\dot\rho2} \quad \boldsymbol{0}_{(N-1)\times1}]$; $\boldsymbol{H}_{\delta\dot\rho1} = [e_x^{jk} \quad e_y^{jk} \quad e_z^{jk}]_{(N-1)\times3} C_{ENU}^{ECEF}$; $\boldsymbol{H}_{\delta\dot\rho2} = [0 \quad -c]_{(N-1)\times2}$; $V_{\delta\dot\rho} = [-\upsilon_{\delta\dot\rho}]_{(N-1)\times1}$; $N{\geq}2$.

The measurement equation of depth difference is:

$$\boldsymbol{Z}_P = \boldsymbol{H}_P\boldsymbol{X} + \boldsymbol{V}_P \qquad (30)$$

$$h_I - h_p = (h + \delta h) - (h + \delta h_p + \upsilon_p) = \delta h - \delta h_p - \upsilon_p \qquad (31)$$

where $\boldsymbol{Z}_P = h_I - h_P$; $\boldsymbol{H}_P = [\boldsymbol{0}_{1\times8} \quad 1 \quad \boldsymbol{0}_{1\times10} \quad -1]$; $\boldsymbol{V}_P$=-υ_P; h_I is the vehicle depth estimated by SINS; h_p is depth measurement by PS; h is a real depth; υ_p is measurement noise of depth.

$\boldsymbol{V} = [\boldsymbol{V}_\rho \quad \boldsymbol{V}_{\dot\rho} \quad \boldsymbol{V}_{\delta\rho} \quad \boldsymbol{V}_{\delta\dot\rho} \quad \boldsymbol{V}_P]^T$ is the measurement noise associated with measurement errors, such as slant range errors, slant-range rate errors, slant-range difference errors, slant-range rate difference errors and depth error. For simplicity, $\boldsymbol{V}$ is modelled as a zeros mean white noise sequence, i.e. $\sim\mathcal{N}(0,\boldsymbol{R})$, where $\boldsymbol{R}$ is an invertible covariance matrix.

III. SINS/LBL INTEGRATION AND EXPERIMENTAL SETUP

A. SYSTEM FRAMEWORK

The proposed hybrid tightly-coupled SINS/LBL system consists of SINS, LBL and PS, and the integration framework is depicted in Fig. 2.
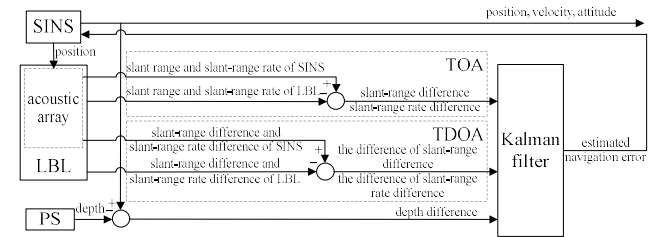

FIGURE 2. Block diagram showing the hybrid tightly-coupled framework for SINS/LBL

SINS is taken as a primary navigation system in the integrated navigation system. On one hand, the four measurement variables are calculated through the vehicle position estimated by SINS and known hydrophone position in acoustic array. On the other hand, the four measurement variables are calculated by sound velocity, time of arrival, time difference of arrival, phase wavelength and Doppler frequency shift, which are obtained by sound source on the vehicle, acoustic array composed of hydrophones on the seafloor and information processor. The differences between the measurement variables of SINS and those of LBL, as well as the depth difference are input to Kalman filter for information fusion. The navigation errors of SINS are corrected by navigation error estimates which are output of the filter to provide high-accuracy navigation. Especially, the key idea of the new framework is the hybrid model for the estimator's rapid convergence upon reaching the acoustic array area.

B. EXPERIMENTAL SETUP

In order to use test data for evaluating SINS/LBL performance, the proposed hybrid tightly-coupled navigation method is applied to an unmanned surface vehicle (USV) equipped with a low-accuracy inertial measurement unit (IMU), a GPS receiver and an attitude and heading reference system (AHRS). The experimental setup is shown in Fig. 3. The true vehicle track is provided by GPS. The true track is used to validate the achievable navigation performance of the proposed SINS/LBL system.

Table 1 lists used sensors for the USV and performance of the sensors.

FIGURE 3. Experimental setup

TABLE 1. Performance of sensors on the test USV

Sensor errors	Specs
Gyroscope constant drift /((°)·h⁻¹)	1
Gyroscope random walk coefficient /((°)·h⁻¹ᐟ²)	0.2
Accelerometer constant bias /mg	0.2
Accelerometer random walk coefficient /(mg·Hz⁻¹ᐟ²)	0.5
GPS receiver position error /m	10
GPS velocity error /(m/s)	0.1
AHRS yaw error /°	3.5

IV. EXPERIMENTS AND RESULTS

The vehicle obtains its initial position through GPS. The true vehicle track from A to B is illustrated in Fig. 4. The acoustic array is composed of four hydrophones, which are fixed at T_0(2700 m, 6500 m, -900 m), T_1(4200 m, 7800 m, -950 m), T_2(4500 m, 5200 m, -1000 m) and T_3(3000 m, 3900 m, -980 m). The underwater sound propagation distance is set to 2500 m. The magenta circle represents the acoustic array area. As can be seen from the relative position relationship between the vehicle trajectory and the acoustic array, the vehicle gradually approaches the acoustic array from a distance, then enters the array area, and finally leaves the area.
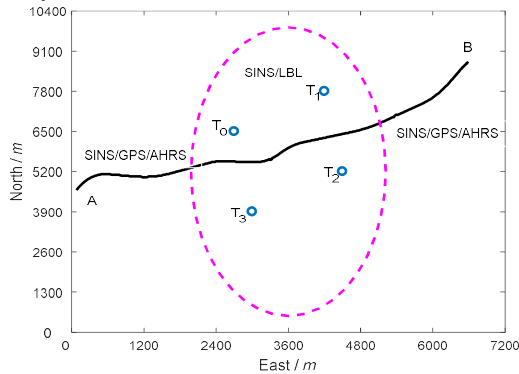

FIGURE 4. The true vehicle track and acoustic array distribution

The integrated navigation modes of the vehicle at different time are shown in Fig. 4. The SINS/GPS/AHRS integrated navigation system is employed when the USV is out of the acoustic array area. It is necessary to note that GPS here is employed for velocity-aided SINS. To validate the effectiveness of the proposed method, when the USV is in acoustic array area, the USV navigation system is changed to SINS/LBL if the number of available hydrophones is more than one. Meanwhile, the GPS-aided and AHRS-aided navigation systems will be turned off to

simulate the situation that they are unavailable. The assistant of GPS and AHRS for integrated navigation system will be turned on again when the vehicle is out of the area.

On the surface, the depth of the USV is 0 m, and the depth error is set to 1 m. In addition, as discussed in Section 1, the time synchronization error between the sound source and the hydrophone is critical for the TOA, and the time synchronization error between the hydrophones is important for the TDOA. Thus, it is assumed that the experiment meets time-synchronized requirements. Additionally, underwater sound velocity is usually measured by a velocity sensor. Here, for an assumed sound velocity of 1500 m/s based on the experimental conditions.

The update periods of SINS and LBL are 10 ms and 1 s, respectively. The vehicle travels about 10 mins. The navigation estimates versus time traveled are shown in Fig. 5. It creates a magnification drawing when there are only two hydrophones available. From the attitude errors in Fig. 5(a), we can see that the proposed hybrid tightly-coupled model has better performance than the slant-range difference model [17], especially in heading estimates.
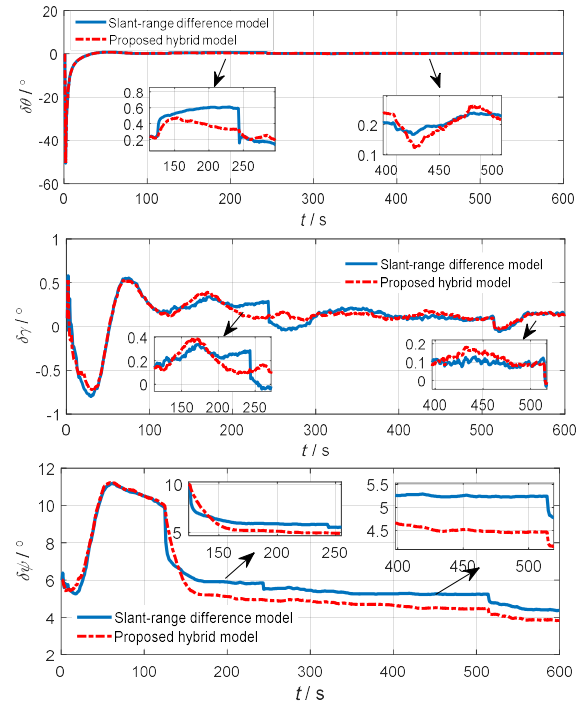
(a) Comparison of attitude error estimates including pitch error $\delta\theta$, roll error $\delta\gamma$ and yaw error $\delta\psi$ from the proposed hybrid model (red, dashed) and the slant-range difference model (blue, solid)
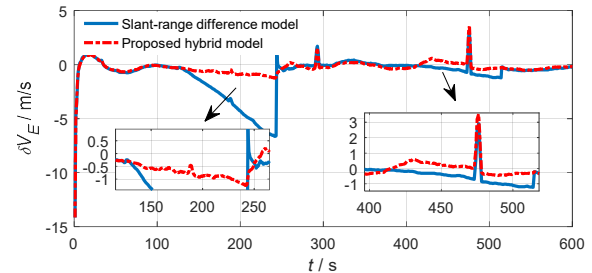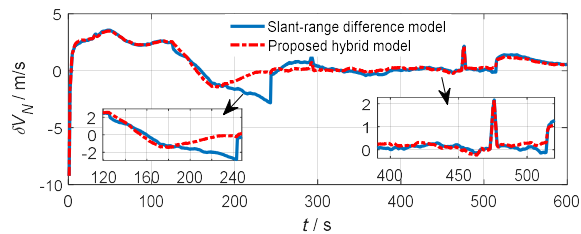
(b) Comparison of velocity error estimates including east velocity error δv_E and north velocity error δv_N from the proposed hybrid model (red, dashed) and the slant-range difference model (blue, solid)

FIGURE 5. Attitude errors and velocity errors of the two tightly-coupled models in SINS/LBL system

As seen in Fig. 5(b), the proposed hybrid model exhibits significantly rapider convergence, specifically between 125s and 242s when there are two hydrophones available.

The position errors of the two tightly-coupled models and the corresponding number of available hydrophones during time traveled are shown in Fig. 6.
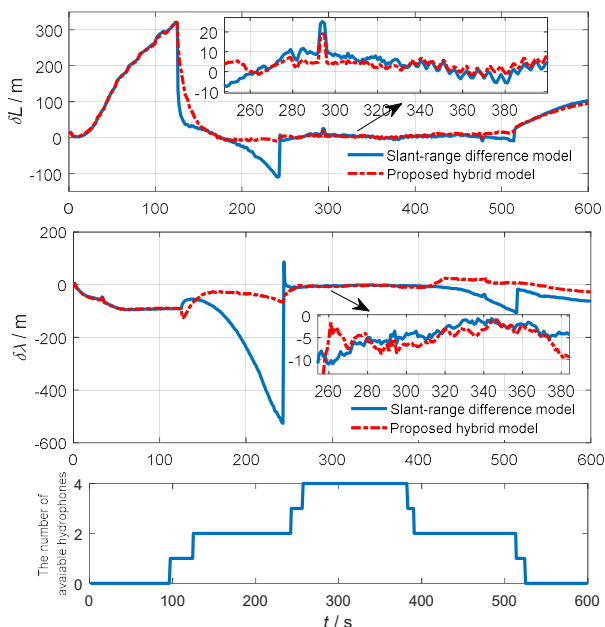

FIGURE 6. Comparison of position error estimates including latitude error δL and longitude error $\delta \lambda$ from the proposed hybrid model (red, dashed) and the slant-range difference model (blue, solid) and the corresponding number of available hydrophones

As can be seen from the comparison of position error estimates in Fig. 6, when the number of available hydrophones is less than two, the position errors of SINS/GPS/AHRS integration are accumulated over time. As the number of available hydrophones increases to two, the integrated navigation system is changed to SINS/LBL, meanwhile, assistant navigation systems from GPS (velocity-aided) and AHRS (heading-aided) are closed. Without GPS and AHRS, the TDOA model (slant-range difference model) shows a significant divergence due to less LBL information. In contrast, more measurement information is incorporated into the estimator, allowing the

hybrid model to help identify and mitigate sensor errors. It takes full advantage of TOA model for faster error convergence and TDOA model for less error overshoot. So the proposed method also shows overall better navigation performance. With an increasing number of available hydrophones, the position error estimates from the proposed hybrid model are commensurate with the slant-range difference model. Table 2 and Table 3 summarize an estimation of the position error for the test results.

TABLE 2. Latitude error δL (*N*=4)

model	Mean /m	standard deviation /m
Slant-range difference model	4.25	5.74
Proposed hybrid model	3.30	3.48

TABLE 3. Longitude error $\delta \lambda$ (*N*=4)

model	Mean /m	standard deviation /m
Slant-range difference model	-4.25	2.78
Proposed hybrid model	-5.08	2.41

When the vehicle drives away from the array area, the navigation errors fluctuate slightly as the number of available hydrophones decreases gradually. Derived from the same principle, attitude errors and velocity errors of the proposed hybrid model tend to divergence more slowly. Its position errors have been improved significantly when the number of available hydrophones is fewer. The navigation system is changed to SINS/GPS/AHRS integrated navigation again when the number of available hydrophones is less than two.

Thus, by the discussion and analysis of the experimental results, it can be seen that the proposed method acquires an improved error convergence and position estimate for USV.

V. CONCLUSIONS

This paper addresses slow navigation error convergence without DVL and MCP information in acoustic array area by the proposed hybrid tightly-coupled SINS/LBL. It adopts slant range, slant-range rate, slant-range difference, slant-range rate difference and depth difference as measurement variables for navigation error correction. The USV test results demonstrate that the proposed method achieves faster error convergence and higher navigation precision, especially when there are fewer than four available hydrophones. It expands the applicability of SINS/LBL methods and makes UVs' trajectory more flexible.

For underwater vehicles in general, the primary source of experimental limitations arises from cost, so the proposed method has not yet been verified under actual field trials. Therefore, if the conditions are met, the method proposed in this paper can be employed in future SINS/LBL systems. In addition, two primary factors i.e. sound velocity and underwater propagation multipath of LBL acoustic signal, will be studied further in the future.

REFERENCES

[1] A. Vasilijevic, D. Nad, F. Mandic, N. Miskovic, and Z. Vukic, "Coordinated navigation of surface and underwater marine robotic vehicles for ocean sampling and environmental monitoring," *IEEE-ASME T. Mech.*, vol. 22, no. 3, pp. 1174-1184, Mar. 2017.

[2] Y. Wu, X. Ta, R. Xiao, Y. Wei, D. An, and D. Li, "Survey of underwater robot positioning navigation," *Appl. Ocean Res.*, vol. 90, Sep. 2019.

[3] P. A. Miller, J. A. Farrell, Y. Zhao, and V. Djapic, "Autonomous underwater vehicle navigation," *IEEE J. Ocean. Eng.*, vol. 35, no. 3, pp. 663-678, Jul. 2010.

[4] J. Quintas, F. Teixeira, and A. Pascoal, "An integrated system for geophysical navigation of autonomous underwater vehicles," *in Proc. the 11th IFAC Conference on Control Applications in Marine Systems*, *Robotics*, *and Vehicles (CAMS)*, Opatija, CROATIA, Sep. 2018, pp. 293-298.

[5] M. Dinc and C. Hajiyev, "Integration of navigation systems for autonomous underwater vehicles," *J. Mar. Eng. Technol.* vol. 14, no. 1, pp. 32-43, May 2015.

[6] R. Ramesh, B. N. Jyothi, N. Vedachalam, G. A. Ramadass Vedachalam, and M. A. Atmanand, "Development and performance validation of a Navigation System for an Underwater Vehicle," *J. Navigation*, vol. 69, no. 5, pp. 1097-1113, Jan. 2016.

[7] O. Hegrenaes, K. Gade, O. K. Hagen, and P. E. Hagen, "Underwater transponder positioning and navigation of autonomous underwater vehicle," *in Proc. OCEANS 2009, MTS/IEEE Bilox-Marine Technology for Our Future: Global and Local Challenges*, Biloxi, MS, USA, Oct. 2009, pp. 26-29.

[8] P. M. Lee, B. H. Jeon, S. M. Kim, H. T. Choi, C. M. Lee, T. Aoki, and T. Hyakudome, "An integrated navigation system for autonomous underwater vehicles with two range sonars, inertial sensors and Doppler velocity log," *in Proc. Oceans '04 MTS/IEEE Techno-Ocean '04 Conference*, Kobe, JAPAN, Nov. 2004, pp. 1586-1593.

[9] P. Lee, B. Jun, K. Kim, J. Lee, T. Aoki, and T. Hyakudome, "Simulation of an inertial acoustic navigation system with range aiding for an autonomous underwater vehicle," *IEEE J. Ocean. Eng.*, vol. 32, no. 2, pp. 327-345, Nov. 2007.

[10] S. E. Webster, M. Eustice, H. Singh, and L. L. Whitcomb, "Advances in single-beacon one-way-travel-time acoustic navigation for underwater vehicles," *Int. J. Robot. Res.* vol. 31, no. 8, pp. 935-950, Jul. 2012.

[11] J. H. Kepper, B. C. Claus, and J. C. Kinsey, "A Navigation Solution Using a MEMS IMU, Model-Based Dead-Reckoning, and One-Way-Travel-Time Acoustic Range Measurements for Autonomous Underwater Vehicles," *IEEE J. Oceanic Eng.*, vol. 44, no. 3, pp. 664-682, Jun. 2018.

[12] Y. Chen, D. Zheng, P. A. Miller, and J. A. Farrell, "Underwater inertial navigation with long baseline transceivers: a near-real-time approach," *IEEE. T. Contr. Syst. T.*, vol. 24, no. 1, pp. 240-251, May 2015.

[13] L. Zhou, X. Cheng, Y. Zhu, C. Dai, and J. Fu, "An effective terrain aided navigation for low-cost autonomous underwater vehicles," *Sensors*, vol. 17, no. 4, Mar. 2017.

[14] P. Liu, B. Wang, Z. Deng, and M. Fu, "INS/DVL/PS tightly coupled underwater navigation method with limited DVL measurements," *IEEE. Sens. J.*, vol. 18, no. 7, pp. 2994-3002, Jan. 2018.

[15] P. Lee, B. Jun, H. Choi, and S. Hong, "An integrated navigation systems for underwater vehicles based on inertial sensors and pseudo LBL acoustic transponders," *in Proc. Oceans 2005 Conference*, Washington, DC, USA, Sep. 2005, pp. 555-562.

[16] P. Lee, B. Jun, S. Hong, Y. Lim, and S. Yang, "Pseudo long base line (LBL) hybrid navigation algorithm based on inertial measurement unit with two range transducers," *J. Ocean Eng. Technol*, vol. 19, no. 5, pp. 71-77, Oct. 2005.

[17] T. Zhang, H. Shi, L. Chen, Y. Li, and J. Tong, "AUV positioning method based on tightly coupled SINS/LBL for underwater acoustic multipath propagation," *Sensors*, vol. 16, no. 3, Mar. 2016.

[18] T. Zhang, L. Chen, and Y. Yan, "Underwater positioning algorithm based on SINS/LBL integrated system," *IEEE Access*, vol. 6, pp. 7157-7163, Jan. 2018.

[19] T. Zhang, L. Chen, and Y. Li. "AUV underwater positioning algorithm based on interactive assistance of SINS and LBL," *Sensors*, vol. 16, no. 1, Jan. 2016.

[20] D. H. Titterton, J. L. Weston, "Strapdown Inertial Navigation Technology," 2nd ed., Reston, VA, USA: American Institute Aeronautics Astronautics, 2004.

LING ZHOU received the B.S. degree in electronic and information engineering and M.S. degree in signal and information processing from North University of China, Taiyuan, China, in 2003 and 2006, and Ph.D. degree in instrument science and technology from Southeast University, Nanjing, China, in 2018. During her Ph.D., she was a full-time graduate student in Key Laboratory of Micro-Inertial Instrument and Advanced Navigation, researching inertial navigation and integrated navigation. In addition, she was also involved in information fusion technology. She is currently a lecturer in Department of Physics and Electronic Engineering at Yuncheng University. Her current research interests include the design of acoustic navigation for autonomous underwater vehicles.
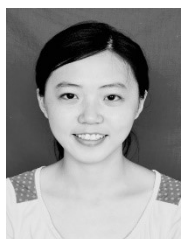
YIXIAN ZHU received the B.S. degree in measuring and controlling technology and instrument from Nanjing University of Technology, Nanjing, China, in 2011, and combined M.S. and Ph.D. degree in navigation, guidance and control from Southeast University, Nanjing, China, in 2018. During her Ph.D., she was a full-time graduate student in Key Laboratory of Micro-Inertial Instrument and Advanced Navigation, researching fault detection and tolerance technologies for navigation systems. In addition, she was also involved in information fusion technology. She is currently a lecturer in Department of Materials Science and Engineering at Nantong University. Her current research interests include the design of fault tolerance for autonomous underwater vehicles.